Journal of Magnetic Resonance 198 (2009) 275–281

Contents lists available at ScienceDirect

Journal of Magnetic Resonance

journal homepage: www.elsevier.com/locate/jmr

Communication

H-start for exclusively heteronuclear NMR spectroscopy: The case of intrinsically disordered proteins

Wolfgang Bermel [a], Ivano Bertini [b,*], Veronika Csizmok [c], Isabella C. Felli [b], Roberta Pierattelli [b], Peter Tompa [c]

[a] Bruker BioSpin GmbH, Silberstreifen, 76287 Rheinstetten, Germany
[b] CERM and Department of Chemistry, University of Florence, Via Luigi Sacconi 6, IT-50019 Sesto Fiorentino, Florence, Italy
[c] Institute of Enzymology, Biological Research Center, Hungarian Academy of Sciences, Budapest, Karolina ut 29, H-1113, Hungary

ARTICLE INFO

Article history:
Received 24 December 2008
Revised 23 February 2009
Available online 4 March 2009

Keywords:
^{13}C direct detection
Protonless NMR
Intrinsically disordered proteins
Virtual decoupling
IPAP
Spin-state selection

ABSTRACT

Here, we present a series of exclusively heteronuclear multidimensional NMR experiments, based on ^{13}C direct detection, which exploit the ^{1}H polarization as a starting source to increase the signal-to-noise ratio. This contributes to make this spectroscopy more useful and usable. Examples are reported for a suitable system such as securin, an intrinsically disordered protein of 22 kDa.

1. Introduction

In recent years, evidence has grown that many proteins are completely or partially disordered in their functional state [1–3]. The advantage of lacking a rigid structure may reside in the malleability conferred by flexibility, allowing binding to multiple targets with high specificity and low affinity, which may be a key aspect in intermediate steps of biochemical pathways. Atomic level characterization of the structural and dynamic features of intrinsically disordered proteins may also highlight regions characterized by transient local order which may be important for function. The characterization of unfolded systems is also important to understand processes of folding coupled to binding and, more in general, the energy landscape of proteins. All of these aspects have raised a considerable gain of interest in these systems. Nuclear magnetic resonance spectroscopy (NMR) is the key experimental method for obtaining site-specific information on intrinsically disordered proteins [4–8].

The lack of a rigid 3D structure has several implications on the NMR observables, the most striking being the reduced chemical shift dispersion of the signals that may cause extensive spectral overlap. Therefore it is advisable to focus the NMR experiments on nuclei that retain the largest chemical shift dispersion in disordered ensembles. Protons, which are intrinsically characterized by low chemical shift dispersion, are the least indicated in terms of enhancing the spectral resolution whereas ^{13}C and ^{15}N are more suitable. Therefore, *exclusively heteronuclear multidimensional* NMR experiments are in principle the ideal choice to study unfolded proteins. The known drawback of these experiments is the intrinsic low sensitivity [9]. The sensitivity can be significantly improved by exploiting the ^{1}H polarization as a starting point of the NMR experiments [10–12]. This can be profitably implemented in many of the available *protonless* NMR experiments and enables the design of additional ones. We show here several examples of exclusively heteronuclear NMR experiments with improved sensitivity and resolution. The improvement in sensitivity is mainly due to the use of ^{1}H as a starting polarization source while the improvement in resolution comes from frequency labelling of heteronuclear chemical shifts in all the dimensions of the NMR experiments as well as from a new virtual decoupling method of carbonyl carbons. Although generally applicable, these experiments are particularly well suited for the characterization of intrinsically disordered proteins, as here demonstrated on human securin, an intrinsically disordered protein of 22.2 kDa [13].

2. Results and discussion

The CBCACON experiment, a C′-detected experiment which proved useful for the identification of spin-systems in intrinsically disordered proteins [7], can be taken as an example to show the

* Corresponding author. Fax: + 39 055 4574271.
E-mail address: ivanobertini@cerm.unifi.it (I. Bertini).

1090-7807/$ - see front matter © 2009 Elsevier Inc. All rights reserved.
doi:10.1016/j.jmr.2009.02.012

improvement in sensitivity obtained by exploiting the ^{1}H polarization as a starting point of the NMR experiments through an INEPT-type transfer [10]. The gain in sensitivity obtained with the modified pulse sequence (H)CBCACON (described in Appendix, Panel 1) applied to a 0.7 mM sample of human securin, is approximately 2.2 (Fig. 1A and B), which implies a reduction in experimental time of a factor of about 4.8 compared to the standard CBCACON experiment [14,15]. The observed gain in sensitivity is smaller than that expected simply considering the gyromagnetic ratios of the nuclei providing the starting polarization. Among the reasons for the reduced gain, the following are important: 1) the necessity to compromise in the choice of the optimal delay for the refocused INEPT transfer step to detect ^{13}C signals with a different number of directly attached protons (CH, CH_2, CH_3) [16–18], and 2) the proton and carbon relaxation occurring during the INEPT transfer step itself.

It is worth noting that the 3D (H)CBCACON experiment is still an exclusively heteronuclear experiment, with C′, C^{ali} and N labelled in the three dimensions, and it can be recorded with high-resolution (Fig. 1C, 4 scans per increment) in 21 h. Selected strips of the very same 3D map are reported in Fig. 2.

The use of ^{1}H polarization as a starting point in exclusively heteronuclear NMR experiments permits also to expand the series of experiments for protein sequence specific assignment. In particular novel CANCO [19] variants can be designed starting with H–C or H–N INEPT-type transfer steps (Appendix, Panels 2 and 3). In Fig. 2 selected strips from the 3D (H)CBCANCO and the 3D (H)NCANCO are shown. The (H)CBCANCO experiment, which besides the C^{α}_{i},N_{i+1}, C'_{i} and C^{α}_{i+1},N_{i+1}, C'_{i} correlations present in the CANCO encodes the information on the C^{β}_{i} and C^{β}_{i+1} chemical shifts, links in a sequence specific manner the spin-systems identified with the (H)CBCACON. The (H)NCANCO enables the correlation of each backbone carbonyl (C'_{i}) with three backbone nitrogens (N, i.e. N_i, N_{i+1}, and N_{i+2}), providing an additional means to perform the complete sequence specific assignment of the polypeptidic chain. The latter experiment would not have been possible without the ^{1}H-start as, in fact, the signal-to-noise ratio of the spectrum obtained with a pulse sequence starting on nitrogen would have been very low, making this experiment useless in practice.

Thus, a couple of experiments provide the complete chemical shift assignment for C′, C^{α}, C^{β}, and N nuclei in human securin, including prolines. In an intrinsically disordered protein these data are highly valuable *per se*, as the deviations of the experimental chemical shift values from the random-coil values are indicators of local structural propensity [20,21] that can be analyzed and interpreted on biochemical grounds.

To complete the NMR characterization of the structural and dynamic properties of a protein it is often necessary to determine ^{15}N and/or ^{13}C relaxation rates, exchange rates with the solvent, residual dipolar couplings, etc. These observables, which are generally measured through variants of HN HSQC experiments, can be determined with variants of the CON experiment, which can be modified with the inclusion of the H-start building block. An example is given by the C′–N correlation experiment to measure H^{N}–N residual dipolar couplings in human securin (Appendix, Panel 5). This experimental scheme, taking advantage of the large chemical shift dispersion provided by heteronuclear chemical shifts (C′ and N) and of the increased sensitivity provided by the proton-polarization, allowed a considerable increase in the number of residues for which residual dipolar couplings could be measured with respect to the standard HSQC-type experiments based on direct detection of H^{N} (i.e. passing from 90 [13] to 162 residues, not shown). With a similar approach all the experiments to determine coupling constants and relaxation rates can be implemented.

The outcome of the experiments based on carbonyl direct detection is very sensitive to the performance of C′–C^{α} homonuclear decoupling and the use of spin-state selective variants were shown to be very effective in the removal of the homonuclear splittings [14,22,23]. Among them the IPAP method was implemented in all the experiments described above and was key to obtaining the high-resolution needed. Along the same lines, also the C′–N coupling can be eliminated including a sensitivity-improved IPAP scheme [24], as described in the experimental part and in the Appendix (Panel 5). This new variant of virtual decoupling of C′ carbons from C^{α} and N, called SE-DIPAP, does not require ^{15}N RF irradiation, which usually limits the duration of the acquisition time. In the case of unfolded proteins this is particularly useful as the FID can be sampled as long as needed. The results obtained on human securin are shown in Fig. 3 and demonstrate the improved resolution that can be obtained for carbonyl signals.

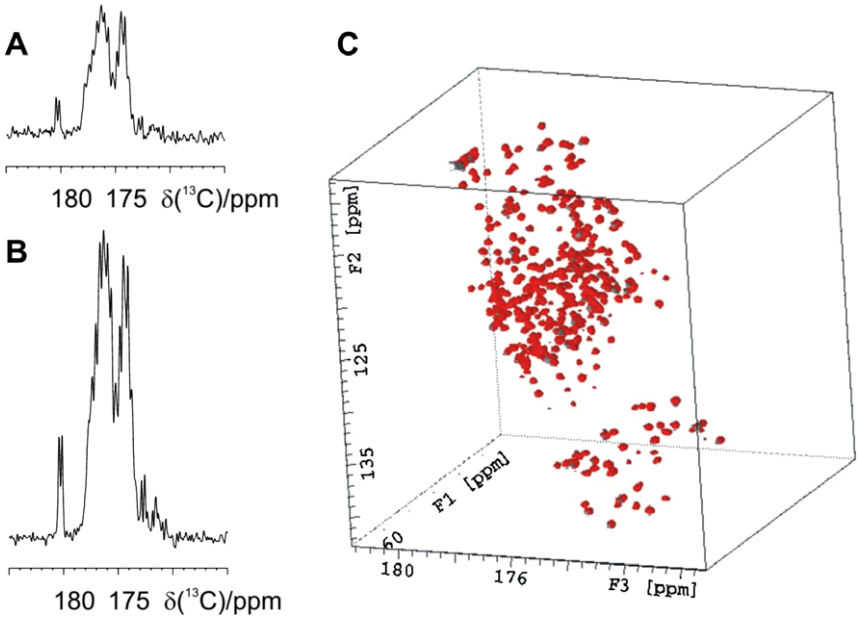

Fig. 1. Increase in sensitivity obtained by using the ^{1}H polarization as a starting pool in a C′-detected experiment. As an example, the first FID of the CBCACON (A) and (H)CBCACON (B) recorded on a 0.7 mM human securin sample are shown. The full 3D experiment recorded with 96 × 144 increments in the two indirect dimensions is also reported (C).

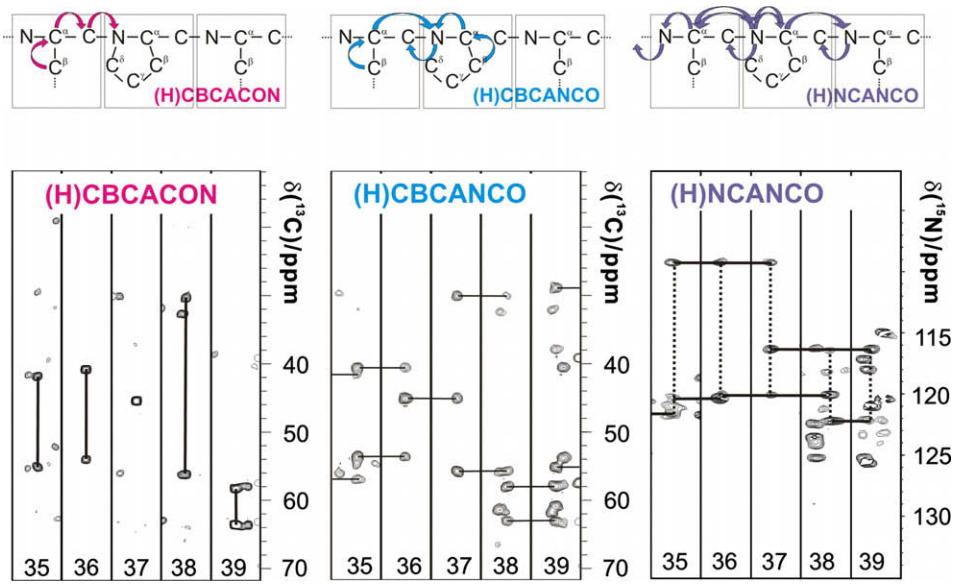

Fig. 2. Representative slices of $^{13}C^{ali}$–$^{13}C'$ planes at specific ^{15}N resonances taken from the (H)CBCACON and (H)CBCANCO spectra as well as slices of ^{15}N–$^{13}C'$ planes at specific ^{15}N resonances taken from the (H)NCANCO spectrum of ^{13}C–^{15}N-labelled human securin at 281.6 K. In the (H)CBCACON for each residue the C_i^{α}–C'_i–N_{i+1} and, for non-Gly residues, the C_i^{β}–C'_i–N_{i+1} correlations are present. In the (H)CBCANCO the C_{i+1}^{α}–C'_i–N_{i+1} and C_{i+1}^{β}–C'_i–N_{i+1} correlations are also present. In the (H)NCANCO each C'_i–N_{i+1} is correlated with the N_i and N_{i+2} nuclei. The residue number is indicated at the bottom of each slice (C'_i). The magnetization transfer pathways for the three experiments are also schematically reported top of each experiment.

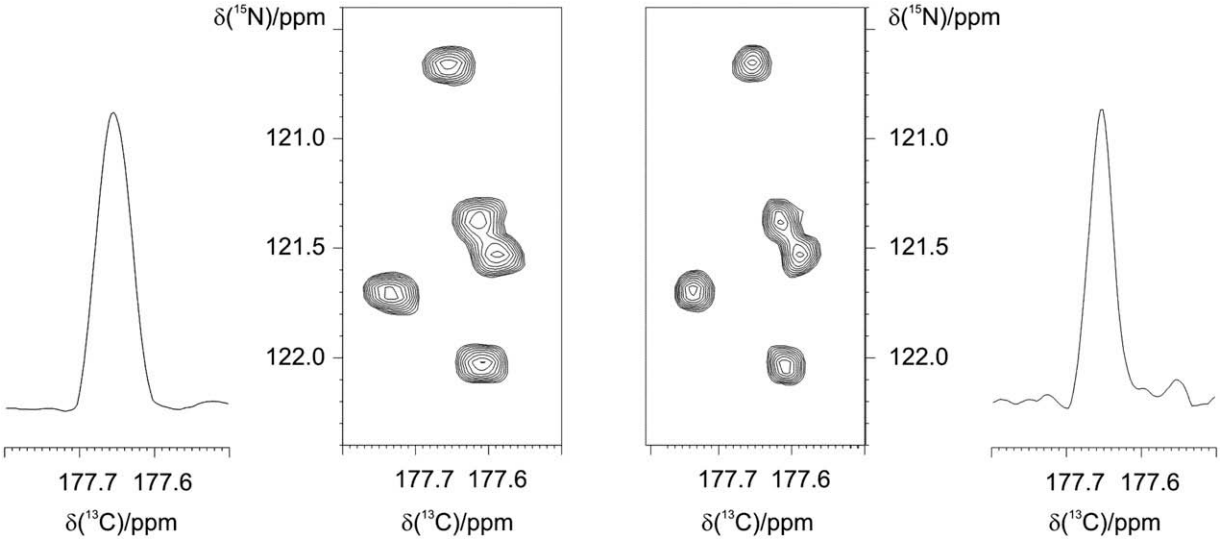

Fig. 3. The new variant of spin-state-selective virtual decoupling of carbonyls during the direct acquisition dimension (SE-DIPAP), based on including C'–N virtual decoupling in the experiment (CON in the present case), in addition to the C'–C^{α} virtual decoupling, is demonstrated here by comparing it with the standard IPAP version for C'–C^{α} virtual decoupling. A portion of the 2D CON maps and the trace of the upper cross peak for the left IPAP version and right the new SE-DIPAP variant are shown.

3. Conclusions

Carbon-13 direct detected experiments are amenable to perform the complete NMR characterization of a protein, warranting high chemical shift dispersion in the NMR spectra. This is particularly important for the study of systems of increasing complexity such as large intrinsically disordered proteins. The limitation posed by sensitivity can be overcome, as here demonstrated, with the exploitation of proton-polarization as a starting pool.

4. Experimental

The ^{13}C, ^{15}N labelled human securin sample was prepared and purified as previously reported [13]. The protein concentration was 0.7 mM in 25 mM phosphate buffer, 150 mM KCl pH 7.2, 10 mM $HSCH_2CH_2OH$. In all cases 10% D_2O was added to the sample for the lock signal.

Carbon-13 direct detection experiments were carried out on a 16.4 T Bruker AVANCE 700 spectrometer, operating at 700.06 MHz for ^1H and 176.03 MHz for ^{13}C and equipped with a TXO ^{13}C, ^{15}N, ^1H cryogenically cooled probe. All spectra were recorded at 281.6 K.

The pulse sequences to acquire the experiments outlined in the main text as well as the experimental parameters used are described in the Appendix. All pulses were given with phase x, unless otherwise specified. In all the panels reported, unless otherwise specified, band selective ^{13}C pulses are denoted by shapes and rectangular pulses represent hard pulses. The wide and narrow pulses

correspond to π and π/2 flip angles. Pulse field gradients (PFG line) are also indicated by shapes. The common parameters used for all experiments are described in detail in this paragraph, while those specific of each experiment are reported in the captions to the different panels. Unless otherwise specified, for ^{13}C bandselective π/2 and π flip angle pulses Q5 (or time reversed Q5) and Q3 shapes [25] were used with durations of 274 and 220 μs, respectively except for the π pulse indicated in grey (Q3, 860 ms) and for the π pulse indicated in crossed stripes (adiabatic inversion pulse over the C′ and C^{α} regions, Chirp [26], 500 μs). The ^{1}H and ^{15}N carriers are placed at 4.7 and 125 ppm, respectively. The change in the position of the ^{13}C carrier (39 ppm for C^{ali}, 55 ppm for C^{α}, and 173 ppm for C′, 100 ppm for the adiabatic pulse) is indicated by vertical arrows. Decoupling of the ^{1}H and ^{15}N was achieved with waltz-16 [27] (1.7 kHz) and garp-4 [28] (1.0 kHz), respectively. The relaxation delay was 1.2–1.3 s and acquisition time in the direct dimension was between 60 and 110 ms. The spectral widths were of 50 (C′), 35 (N) and 65 (C^{ali}) ppm. The experiments employ the IPAP approach to suppress the C^{α}-C′ coupling [14] and the in-phase (IP) and anti-phase (AP) components are acquired and stored separately by using the pulse schemes illustrated, doubling the number of FIDs recorded in one of the indirect dimensions. The phase cycle, the method used for quadrature detection, the durations of the delays shown in the pulse sequences and the relative strengths of the gradients used (all gradients had a duration of 1 ms and a sine shape) are reported case-by-case.

The implementation of the SE-DIPAP approach to decouple C′ carbons from C^{α} and N is shown, as an example, for the CON experiment (Appendix, Panel 5). The four independent components (A–D) that are acquired to obtain virtual decoupling of C′ carbons from C^{α} and N through the SE-DIPAP scheme are shown in Fig. 4. The pair of independent FIDs to separate the in-phase and anti-phase components of C′ respect to N are obtained by a 180° phase shift of the last ^{15}N pulse, which causes a change in sign of the anti-phase component (the one generally lost through ^{15}N decoupling), while leaving unaffected the in-phase component. The pair of independent components to detect the in-phase and anti-phase components of C′ respect to C^{α} are obtained by changing the position of the 180° C^{α} pulses to prevent (IP) or allow (AP) C′–C^{α} scalar coupling evolution. As shown

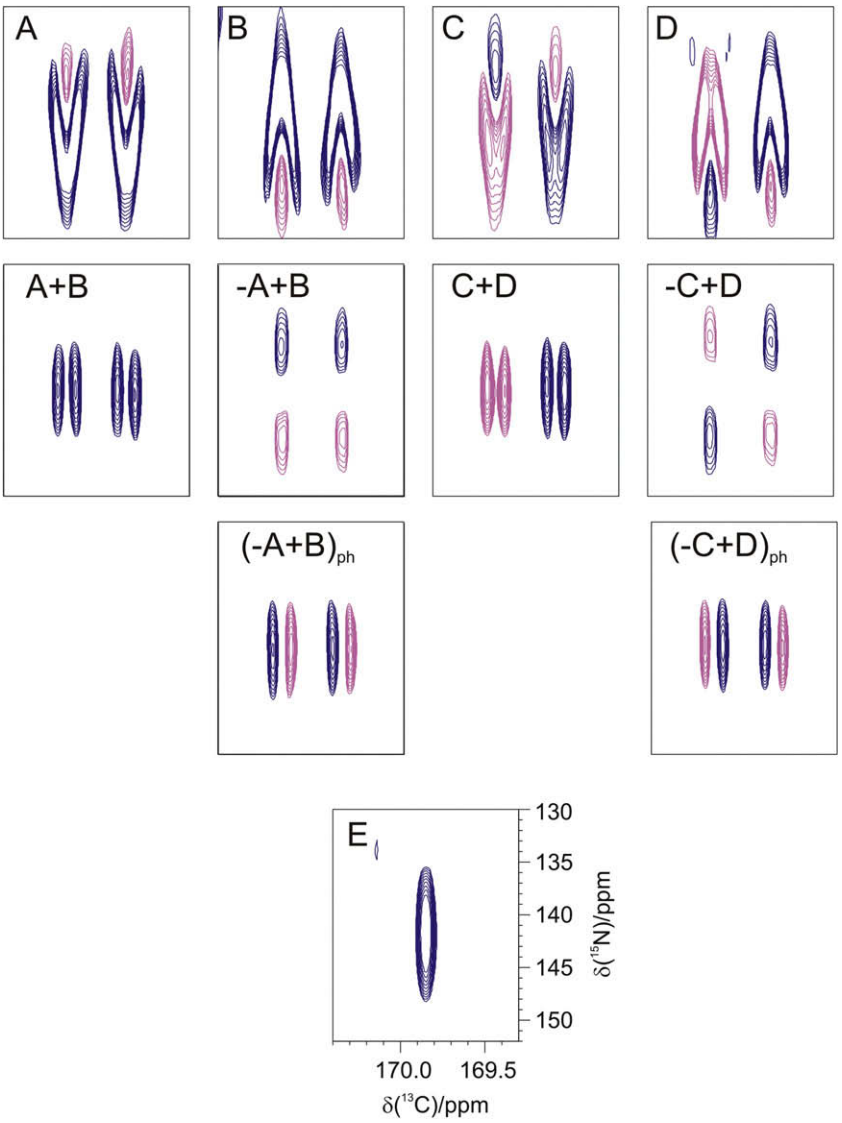

Fig. 4. The four independent components acquired through the SE-DIPAP scheme (A–D) are combined to provide the decoupled signal (E) according to the description reported in the text.

in the figure, (A + B) and (C+D) yield the IP and AP components of C′ respect to C^{α}, with the C′–N coupling in phase. The (−A + B) and (−C + D), after a 90° phase correction in the two dimensions $(-A + B)_{ph}$ and $(-C + D)_{ph}$, give the IP and AP components of C′ respect to C^{α}, with the C′–N coupling in anti-phase. The four independent multiplet components can then be separated by taking the proper linear combinations. Shifting those to the center of the original multiplet and adding them achieves C′ virtual decoupling (E). For the sake of clarity, the data used here to describe the method are acquired on the octapeptide hymenistatin and the C′ (Ile[8])N(Pro[1]) correlation is shown in Fig. 4.

Acknowledgments

This work has been supported in part by the EC contracts EU-NMR No. 026145 and SPINE II No. 031220 and by Ente Cassa di Risparmio di Firenze.

Appendix A

A.1. Panel 1 - (H)CBCACON

The delays are: $\varepsilon = t_2(0)$, $\delta = 3.6$ ms, $\Delta = 9$ ms, $\Delta_1 = 25$ ms, $\Delta_2 = 8$ ms, $\Delta_3 = \Delta_2 - \Delta_4 = 5.8$ ms, $\Delta_4 = 2.2$ ms. The phase cycle is: $\phi_1 = 8(x)$, $8(-x)$; $\phi_2 = x$, $-x$; $\phi_3 = 4(x)$, $4(-x)$; $\phi_4 = 2(x)$, $2(-x)$; $\phi_{IPAP}(IP) = x$; $\phi_{IPAP}(AP) = -y$; $\phi_{rec} = x, -x, -x, x, -x, x, x, -x$. Quadrature detection was obtained by incrementing phase ϕ_2 (t_1) and ϕ_4 (t_2) in a States-TPPI manner. The experiment was acquired with 4 scans, $144 \times 96 \times 1024$ data points in the t_1, t_2 and t_3 dimensions (Panel 1).

A.2. Panel 2 - (H)CBCANCO

The delays are: $\delta = 3.6$ ms, $\Delta = 9$ ms, $\Delta_0 = 32$ ms, $\Delta_1 = 22$ ms, $\Delta_2 = 8$ ms, $\Delta_3 = \Delta_2 - \Delta_4 = 5.8$ ms, $\Delta_4 = 2.2$ ms. The phase cycle is: $\phi_1 = 8(x)$, $8(-x)$; $\phi_2 = y$, $-y$; $\phi_3 = 2(x)$, $2(-x)$; $\phi_{IPAP}(IP) = 4(x)$, $4(-x)$; $\phi_{IPAP}(AP) = 4(-y)$, $4(y)$; $\phi_{rec} = x, -x, -x, x, -x, x, x, -x$. Quadrature detection was obtained by incrementing phase ϕ_2 (t_1) and ϕ_3 (t_2) in a States-TPPI manner. The experiment was acquired with 16 scans, $144 \times 96 \times 1024$ data points in the t_1, t_2 and t_3 dimensions (Panel 2).

A.3. Panel 3 - (H)NCANCO

The delays are: $\delta = 4.6$ ms, $\xi = 5.5$ ms, $\Delta = 9$ ms, $\Delta_1 = 24$ ms, $\Delta_2 = 50$ ms, $\Delta_3 = 32$ ms. The phase cycle is: $\phi_1 = x$, $-x$; $\phi_2 = 4(x)$, $4(-x)$; $\phi_3 = 2(x)$, $2(-x)$; $\phi_{IPAP}(IP) = 8(x)$, $8(-x)$; $\phi_{IPAP}(AP) = 8(-y)$, $8(y)$; $\phi_{rec} = x, -x, -x, x, -x, x, x, -x, -x, x, x, -x, x, -x, -x, x$. Quadrature detection was obtained by incrementing phase ϕ_1 (t_1) and ϕ_3 (t_2) in a States-TPPI manner. The experiment was acquired with 16 scans, $144 \times 96 \times 2048$ data points in the t_1, t_2 and t_3 dimensions (Panel 3).

A.4. Panel 4 - Determination of HN RDCs through a C′–N correlation experiment

The delays are: $\delta = 4.6$ ms, $\delta' = 5.5$ ms, $\Delta = 9$ ms, $\Delta_1 = 24.8$ ms, $\Delta_3 = 24.8$ ms. The phase cycle is: $\phi_1 = x$, $-x$; ϕ_2 (AP NH) = $2(x)$, $2(-x)$; ϕ_2 (IP NH) = $2(-y)$, $2(y)$; $\phi_3 = 8(x)$, $8(-x)$; $\phi_{IPAP}(IP) = 4(x)$, $4(-x)$; $\phi_{IPAP}(AP) = 4(-y)$, $4(y)$; $\phi_{rec} = x, -x, -x, x, -x, x, x, -x$. The two FIDs to separate the in-phase and anti-phase components of the H^N–N splitting are obtained by acquiring two experiments that differ by the application of the grey ^{1}H 180° pulse. Quadrature detection was obtained by incrementing phase ϕ_2 (t_1) in a States-TPPI manner. The experiment was acquired with 4 scans, 2048×2048 data points in the t_1 and t_2 dimensions (Panel 4).

A.5. Panel 5 - Spin-state-selective variant for virtual decoupling of C′ carbons from C^{α} and N (SE-DIPAP)

The delays are: $\varepsilon = t_2(0)$, $\Delta = 9$ ms, $\Delta_1 = 32$ ms. The phase cycle is: $\phi_1 = x$, $-x$; $\phi_2 = 2(x)$, $2(-x)$; $\phi_3 = 4(x)$, $4(-x)$; $\phi_4 = 4(y)$, $4(-y)$; $\phi_{IPAP}(IP) = x$; $\phi_{IPAP}(AP) = -y$; $\phi_{rec} = x, -x, x, -x, -x, x, -x, x$. The two independent components, linear combinations of in-phase and anti-phase coherences of C′ respect to N, are acquired separately with two experiments that differ for the phase of the last ^{15}N pulse (ϕ_4 is incremented by π in the second experiment). This allows to recover both orthogonal components of the ^{15}N signal that has evolved during t_1, avoiding loss of one of the two. The data are then processed to separate the four multiplet components of C′ respect to C^{α} and N, which are then shifted to the center of the original multiplet and summed as described in the Experimental section. Quadrature detection was obtained by incrementing in a States-TPPI manner phase ϕ_1 (t_1) (Panel 5).

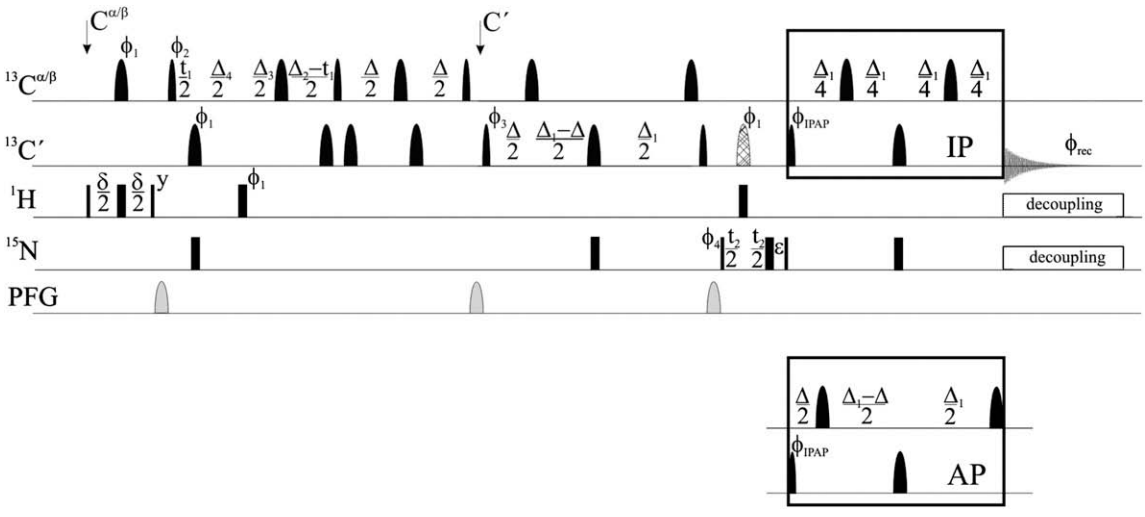

Panel 1.

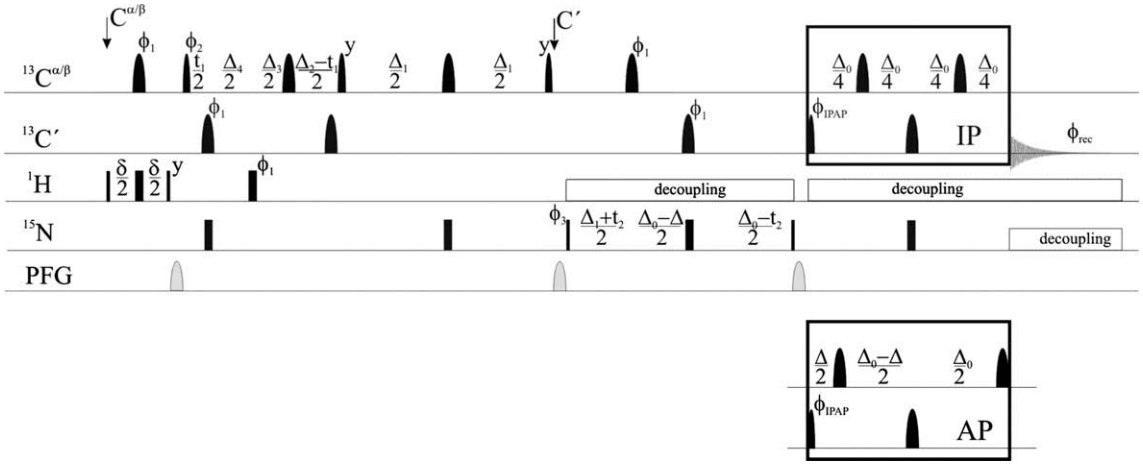

Panel 2.

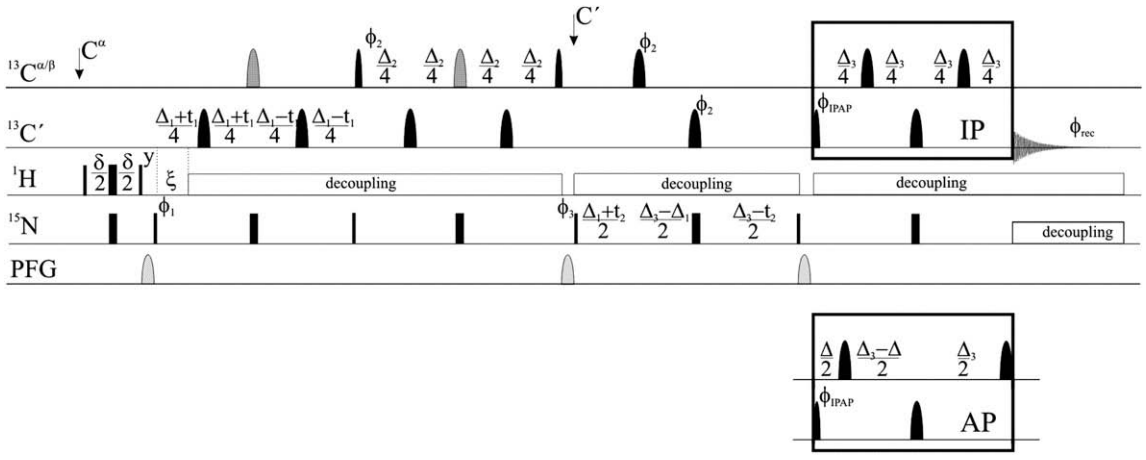

Panel 3.

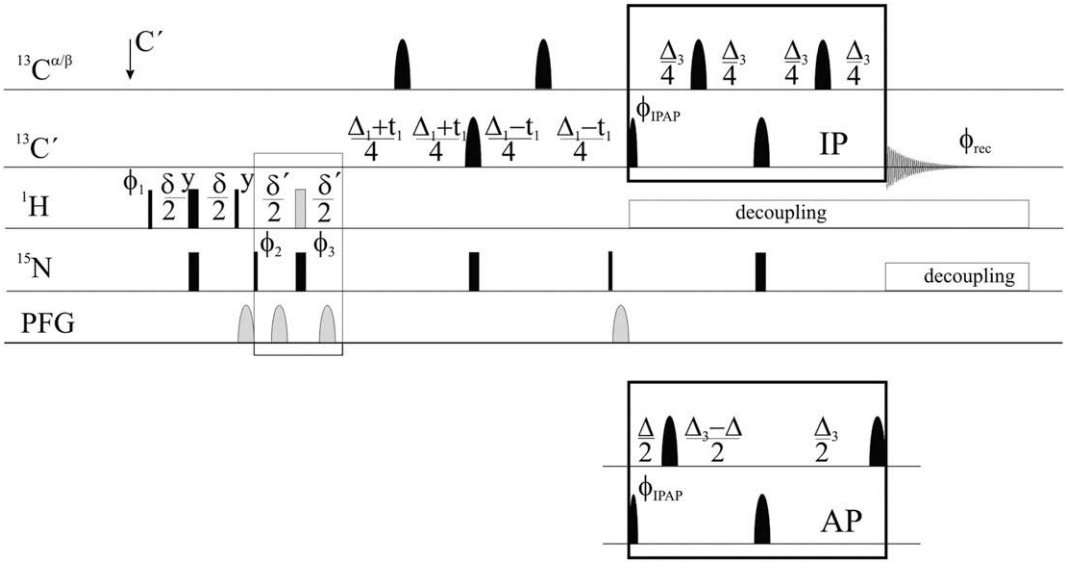

Panel 4.

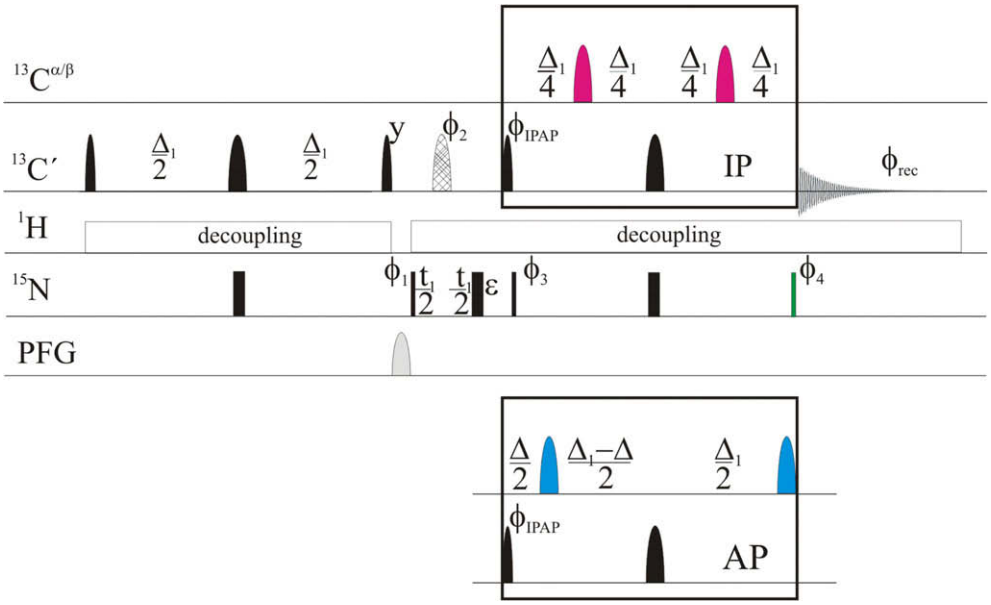

Panel 5.

References

[1] P. Tompa, Intrinsically unstructured proteins, Trends Biochem. Sci. 27 (2002) 527–533.
[2] H.J. Dyson, P.E. Wright, Intrinsically unstructured proteins and their functions, Nat. Rev. Mol. Cell Biol. 6 (2005) 197–208.
[3] M. Sickmeier, J.A. Hamilton, T. LeGall, V. Vacic, M.S. Cortese, A. Tantos, B. Szabo, P. Tompa, J. Chen, V.N. Uversky, Z. Obradovic, A.K. Dunker, DisProt: the database of disordered proteins, Nucleic Acids Res. 35 (2007) D786–D793.
[4] J. Klein-Seetharaman, M. Oikawa, S.B. Grimshaw, J. Wirmer, E. Duchardt, T. Ueda, T. Imoto, L.J. Smith, C.M. Dobson, H. Schwalbe, Long-range interactions within a nonnative protein, Science 295 (2002) 1719–1722.
[5] H.J. Dyson, P.E. Wright, Unfolded proteins and protein folding studied by NMR, Chem. Rev. 104 (2004) 3607–3622.
[6] P. Bernado, C.W. Bertoncini, C. Griesinger, M. Zweckstetter, M. Blackledge, Defining long-range order and local disorder in native a-synuclein using residual dipolar couplings, J. Am. Chem. Soc. 127 (2005) 17968–17969.
[7] W. Bermel, I. Bertini, I.C. Felli, Y.-M. Lee, C. Luchinat, R. Pierattelli, Protonless NMR experiments for sequence-specific assignment of backbone nuclei in unfolded proteins, J. Am. Chem. Soc. 128 (2006) 3918–3919.
[8] T. Mittag, J. Forman-Kay, Atomic-level characterization of disordered protein ensembles, Curr. Opin. Struct. Biol. 17 (2007) 3–14.
[9] W. Bermel, I. Bertini, I.C. Felli, M. Piccioli, R. Pierattelli, ^{13}C-detected *protonless* NMR spectroscopy of proteins in solution, Progr. NMR Spectrosc. 48 (2006) 25–45.
[10] G.A. Morris, R. Freeman, Enhancement of nuclear magnetic resonance signals by polarization transfer, J. Am. Chem. Soc. 101 (1979) 760–762.
[11] L. Müller, Sensitivity enhanced detection of weak nuclei using heteronuclear multiple quantum coherence, J. Am. Chem. Soc. 101 (1979) 4481–4484.
[12] G. Bodenhausen, D.J. Ruben, Natural abundance nitrogen-15 NMR by enhanced heteronuclear spectroscopy, Chem. Phys. Lett. 69 (1980) 185–188.
[13] V. Csizmok, I.C. Felli, P. Tompa, L. Banci, I. Bertini, Structural and dynamic characterization of intrinsically disordered human securin by NMR, J. Am. Chem. Soc. 130 (2008) 16873–16879.
[14] W. Bermel, I. Bertini, L. Duma, L. Emsley, I.C. Felli, R. Pierattelli, P.R. Vasos, Complete assignment of heteronuclear protein resonances by protonless NMR spectroscopy, Angew. Chem. Int. Ed. 44 (2005) 3089–3092.
[15] W. Bermel, I. Bertini, I.C. Felli, R. Kümmerle, R. Pierattelli, Novel ^{13}C direct detection experiments, including extension to the third dimension, to perform the complete assignment of proteins, J. Magn. Reson. 178 (2006) 56–64.
[16] R.R. Ernst, G. Bodenhausen, A. Wokaun, Principles of Nuclear Magnetic Resonance in one and two dimensions, Oxford University Press, London, 1987.
[17] J. Cavanagh, W.J. Fairbrother, A.G. Palmer III, N.J. Skelton, Protein NMR Spectroscopy. Principles and Practice, Academic Press, San Diego, 1996.
[18] D.P. Burum, R.R. Ernst, Net polarization transfer via a J-ordered state for signal enhancement of low-sensitivity nuclei, J. Magn. Reson. 39 (1980) 163–168.
[19] I. Bertini, L. Duma, I.C. Felli, M. Fey, C. Luchinat, R. Pierattelli, P.R. Vasos, A heteronuclear direct detection NMR experiment for protein backbone assignment, Angew. Chem. Int. Ed. 43 (2004) 2257–2259.
[20] H. Zhang, S. Neal, D.S. Wishart, RefDB: a database of uniformly referenced protein chemical shifts, J. Biomol. NMR 25 (2003) 173–195.
[21] S. Schwarzinger, G.J.A. Kroon, T.R. Foss, J. Chung, P.E. Wright, H.J. Dyson, Sequence-dependent correction of random coil NMR chemical shifts, J. Am. Chem. Soc. 123 (2001) 2970–2978.
[22] W. Bermel, I.C. Felli, R. Kümmerle, R. Pierattelli, ^{13}C direct-detection biomolecular NMR, Concepts Magn. Reson. 32A (2008) 183–200.
[23] W. Bermel, I.C. Felli, M. Matzapetakis, R. Pierattelli, E.C. Theil, P. Turano, A method for C^{α} direct-detection in protonless NMR, J. Magn. Reson. 188 (2007) 301–310.
[24] T. Kern, P. Schanda, B. Brutscher, Sensitivity-enhanced IPAP-SOFAST-HMQC for fast-pulsing 2D NMR with reduced radiofrequency load, J. Magn. Reson. 190 (2008) 333–338.
[25] L. Emsley, G. Bodenhausen, Gaussian pulse cascades: new analytical functions for rectangular selective inversion and in-phase excitation in NMR, Chem. Phys. Lett. 165 (1990) 469–476.
[26] J.-M. Boehlen, G. Bodenhausen, Experimental aspects of chirp NMR spectroscopy, J. Magn. Reson. Ser. A 102 (1993) 293–301.
[27] A.J. Shaka, J. Keeler, R. Freeman, Evaluation of a new broadband decoupling sequence. WALTZ-16, J. Magn. Reson. 53 (1983) 313–340.
[28] A.J. Shaka, P.B. Barker, R. Freeman, Computer-optimized decoupling scheme for wideband applications and low-level operation, J. Magn. Reson. 64 (1985) 547–552.